Novel model of a AlGaN/GaN high electron mobility transistor based on an artificial neural network*

Cheng Zhi-Qun(程知群)[a)b)†], Hu Sha(胡 莎)[a)], Liu Jun(刘 军)[a)], and Zhang Qi-Jun[b)]

[a)] *Key Laboratory of Radio-Frequency Circuit and System, Hangzhou Dianzi University, Hangzhou* 310018, *China*
[b)] *Department of Electronics, Carleton University, Ottawa, K1S 5B6, Canada*

(Received 30 August 2010; revised manuscript received 18 October 2010)

In this paper we present a novel approach to modeling AlGaN/GaN high electron mobility transistor (HEMT) with an artificial neural network (ANN). The AlGaN/GaN HEMT device structure and its fabrication process are described. The circuit-based Neuro-space mapping (neuro-SM) technique is studied in detail. The EEHEMT model is implemented according to the measurement results of the designed device, which serves as a coarse model. An ANN is proposed to model AlGaN/GaN HEMT based on the coarse model. Its optimization is performed. The simulation results from the model are compared with the measurement results. It is shown that the simulation results obtained from the ANN model of AlGaN/GaN HEMT are more accurate than those obtained from the EEHEMT model.

Keywords: AlGaN/GaN high electron mobility transistor, modeling, artificial neural network
PACS: 61.72.uj, 73.40.Kp, 07.05.Tp **DOI:** 10.1088/1674-1056/20/3/036106

1. Introduction

GaN as the third kind of typical semiconductor material has been widely investigated for several years due to its wide gap and high breakdown field. AlGaN/GaN high electron mobility transistor (HEMT) appears as a promising candidate for the next generation of wireless communication.[1−3] Computer-aided design (CAD) technique has become an important and necessary tool for designing circuits and systems. So, AlGaN/GaN HEMT as an actively developing device needs to be accurately modeled, thereby designing the circuits and systems correctly. Artificial neural network as an excellent algorithm has been applied to the research on plasma density, plasma distribution[4,5] and so on. In recent years, artificial neural network[6] and space mapping (SM)[7,8] have gained recognition as two important developments addressing the growing computational challenges in modeling, simulation, and optimization in the microwave CAD area. Artificial neural networks (ANNs) can automatically learn the electromagnetic (EM) and physical behaviours in a satisfactory accuracy, and the trained ANN model is applicable to the commercial circuit simulator (Agilent ADS). Measurement results can be used to learn EM and physical behaviours and develop the model even when component formulas are unavailable.[7−9] Trained ANNs can be used to design high-level circuits and systems, allowing fast simulation and optimization. On the other hand, space mapping is an advanced optimization concept, allowing expensive EM optimizations or device behaviour simulations to be performed efficiently with the help of fast but coarse or surrogate models. Recently, an SM-based neuro modeling technique combining neural networks with SM is developed, which uses neural networks to map a coarse model into a fine model. The technique can be applied to passive modeling, small-signal device modeling and large-signal nonlinear modeling, to achieve fast and accurate models for components such as bends, high-temperature superconductor filters, embedded passives in multilayer printed circuits and other linear components.

As we know, Agilent ADS software provides some models, such as the Materka model, Statz model, Curtice model, Gummel-Poon model and EEHEMT model, where the EEHEMT model has become a conventional model for HEMTs such as GaAs HEMTs. In the present paper, we use an EEHEMT model of AlGaN/GaN HEMT as a coarse model. Then a novel ANN model of AlGaN/GaN HEMT based on the coarse model (the EEHEMT model) is used to increase its accuracy. Simulation results from the EEHEMT modeling and ANN modeling are given and compared with the measured data. Comparison results show that the ANN model is more accurate than

*Project supported by the National Natural Science Foundation of China (Grant No. 60776052).
†Corresponding author. E-mail: zhiqun@hdu.edu.cn
© 2011 Chinese Physical Society and IOP Publishing Ltd

the EEHEMT model for AlGaN/GaN HEMT. It is the first time that an ANN has been applied to AlGaN/GaN HEMT modeling with multi biases.

2. Device structure and fabrication

The device in this study is grown on a SiC substrate. The epitaxial layer consists of a 1.5 μm undoped GaN buffer layer, a 1 nm AlN spacer layer, a 4 nm low Al doped $Al_{0.04}Ga_{0.96}N$ layer, and a 20 nm $Al_{0.27}Ga_{0.73}N$ barrier layer. The device is a 0.3 μm long and 200 μm (100×2) wide T-shape GaN HEMT. An average electron mobility of 1800 $cm^2/(V \cdot s)$ and a sheet carrier density of 1.0×10^{13} cm^{-2} are obtained by the room-temperature Hall measurement. In our previous papers,[2,3] we have reported in detail the design process and the advantage of the novel structure of the AlGaN/GaN HEMT.

The GaN HEMT fabrication starts with metalizing the drain and the source by high-vacuum evaporation. The Ohmic contacts are formed by depositing the metal Ti/Al/Ti/Au and then rapid thermal annealing (RTA) at 870 °C for 50 s in N_2 ambient. These steps result in a low ohmic contact resistivity of 0.6 $\Omega \cdot$mm. Si_3N_4 film used for passivation is grown by plasma-enhanced chemical vapour deposition (PECVD). Then, the T-shape Schottky gate is formed by Ni/Au evaporation and subsequent lift-off. Figure 1 shows the proposed AlGaN/GaN HEMT with a gate length of 0.3 μm and gate width of 2×80 μm. The measured data will be given to be compared with the simulated results.

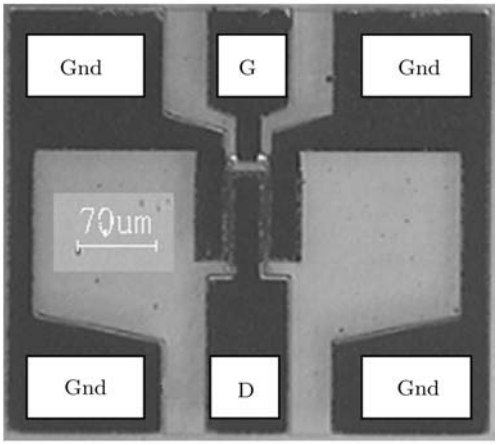


Fig. 1. Diagram of fabricated AlGaN/GaN HEMT. Symbols of G, D and Gnd denote the gate, the drain and the ground respectively.

3. Circuit-based neuro-SM technique

The neuro-SM technique can be used in the case where the existing/available device model cannot match the data of a new device. Let the existing/available nonlinear device model be the coarse model, and let the fine model be a model embodied by the actual device data obtained in the measurements or the detailed/expensive device simulation. Suppose that the gap between the coarse model and the fine model cannot be overcome by simply optimizing the parameters in the coarse model. To obtain a model that can best match the device data, the model structure or the nonlinear equations of the coarse model need to be modified. Figure 2 shows a two-port circuit-based neuro-SM. Let the terminal voltage and the terminal current signals of the coarse model be $\boldsymbol{v}_c = [v_{c1}, v_{c2}]^T$ and $\boldsymbol{i}_c = [i_{c1}, i_{c2}]^T$ respectively. Let the terminal voltage and the terminal current signals of the fine model be $\boldsymbol{v}_f = [v_{f1}, v_{f2}]^T$ and $\boldsymbol{i}_f = [i_{f1}, i_{f2}]^T$ respectively. Here, $\boldsymbol{v}_c$ and $\boldsymbol{i}_c$ are called coarse signals, while $\boldsymbol{v}_f$ and $\boldsymbol{i}_f$ are named fine signals. The fine voltage signal $\boldsymbol{v}_f$ is not sent to the coarse model directly. Instead, it is mapped into the voltage signal $\boldsymbol{v}_c$ in such a way that the modified coarse model response $\boldsymbol{i}_c$ will match the fine output signal $\boldsymbol{i}_f$. Since the accurate equation for the mapping is unknown and the mapping can be nonlinear in general, the neural network is used as a logical representation for the mapping. The input neurons of the neural network receive the fine voltage signal $\boldsymbol{v}_f$. The output neurons provide the mapped voltage signals to the coarse model, i.e., $\boldsymbol{v}_c = \boldsymbol{f}_{ANN}(\boldsymbol{v}_f, \boldsymbol{w})$, where $\boldsymbol{f}_{ANN}$ represents a multilayer feedforward neural network, and $\boldsymbol{w}$ is a vector containing all internal synaptic weights of the neural network. The neural network functions as a voltage-controlled voltage source. A current-controlled current source is used to pass $\boldsymbol{i}_c$ to $\boldsymbol{i}_f$.

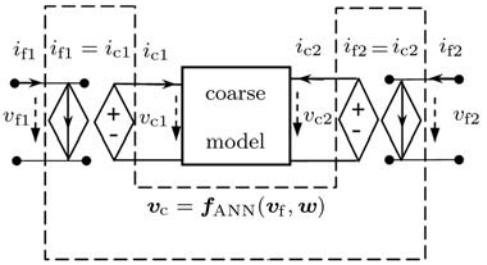


Fig. 2. Structure of a general 2-port neuro-SM nonlinear model. A neural network $\boldsymbol{f}_{ANN}$ is used to provide the mapping between the coarse input signal $\boldsymbol{v}_c$ and the fine input signal $\boldsymbol{v}_f$. Neural network equations act as controlled sources for mapping.

The mapping from the coarse direct current (DC) voltage signal $\boldsymbol{V}_{\rm c,DC}$ to the fine DC voltage signal $\boldsymbol{V}_{\rm f,DC}$ is directly achieved by the neural network. Let the DC response of the neuro-SM model be $\boldsymbol{I}_{\rm f}$. The neuro-SM requires that after receiving the modified signal, the coarse model output signal should become a signal approximate to the fine output signal. Thus, the DC output current of the analytical neuro-SM model as a function of fine DC input voltage signal $\boldsymbol{V}_{\rm f,DC}$ is

$$\boldsymbol{I}_{\rm f} = \boldsymbol{I}_{\rm f}(\boldsymbol{V}_{\rm f,DC}) = \boldsymbol{I}_{\rm c}|_{\boldsymbol{V}_{\rm c,DC}} = \boldsymbol{f}_{\rm ANN}(\boldsymbol{V}_{\rm f,DC}, \boldsymbol{w}). \quad (1)$$

The small-signal scattering-parameters (S-parameters), which are the elements of a scattering matrix, are mapped via the analytical mapping of the $\boldsymbol{Y}$ matrices as

$$\boldsymbol{Y}_{\rm f} = \boldsymbol{Y}_{\rm c}|_{\boldsymbol{V}_{\rm c,Bias}} = \boldsymbol{f}_{\rm ANN}(\boldsymbol{V}_{\rm f,Bias}, \boldsymbol{w}) \times \left(\frac{\partial \boldsymbol{f}^{\rm T}_{\rm ANN}(\boldsymbol{V}_{\rm f}, \boldsymbol{w})}{\partial \boldsymbol{V}_{\rm f}}|_{\boldsymbol{V}_{\rm f}=\boldsymbol{V}_{\rm f,Bias}}\right)^{\rm T}, \quad (2)$$

where $\boldsymbol{Y}_{\rm c}$ is evaluated at the mapped bias $\boldsymbol{V}_{\rm c,Bias}$, and the derivative of $\boldsymbol{f}_{\rm ANN}$ is obtained at the bias of the fine model $\boldsymbol{V}_{\rm f,Bias}$ using the adjoint neural network method. Notice that $\boldsymbol{Y}_{\rm c}$ is complex and has contributions from all elements in the transformation (mapping) of $\boldsymbol{Y}_{\rm c}$.

4. Structure of neuro-SM

Figure 3 shows the structure of the three-layer neural network used in the above circuit-based neuro-SM for AlGaN/GaN HEMT modeling. Let $\boldsymbol{x}$ be a 4-vector containing parameters of a given device, e.g., $\boldsymbol{v}_{\rm f}$ in Fig. 2, which contains gate voltage $V_{\rm g}$, drain voltage $V_{\rm d}$, gate voltage derivative $V'_{\rm g}$ and drain voltage derivative $V'_{\rm d}$ of the fine model. Let $\boldsymbol{y}$ be a 2-vector representing various responses of the device under consideration, e.g., gate voltage $\bar{V}_{\rm g}$ and drain voltage $\bar{V}_{\rm d}$ of the coarse model. The relationship between $\boldsymbol{x}$ and response $\boldsymbol{y}$ is multidimensional and nonlinear. To model such a nonlinear relationship, the three-layer neural network is employed. The input layer and the output layer correspond to device input $\boldsymbol{x}$ and output response $\boldsymbol{y}$ respectively. The hidden layer is represented by a vector $\boldsymbol{z}$. Let

$$\boldsymbol{v}_{\rm f} = \left[V_{\rm g}, V_{\rm d}, V'_{\rm g}, V'_{\rm d}\right]^{\rm T}, \quad (3)$$

and

$$\boldsymbol{v}_{\rm c} = \left[\bar{V}_{\rm g}, \bar{V}_{\rm d}\right]^{\rm T} \quad (4)$$

be vectors representing the inputs and outputs respectively. The weighting factors are w_{ih} between the input and the hidden layers, and v_{hj} between the hidden and the output layers, where $i = 1, 2, 3, 4; h = 1, 2, \ldots, 24$; and $j = 1, 2$. The output from the neural network can be computed as

$$y_j = \sum_{h=1}^{24} z_h v_{hj}, \quad (5)$$

where z_h is a function defined as

$$z_h = f(\gamma_h) = \frac{1}{1 + {\rm e}^{-\gamma_h}}, \quad (6)$$

$$\gamma_h = \left(\sum_{i=1}^{4} x_i w_{ih}\right) + \theta_h, \quad (7)$$

with θ_h being the threshold value for the h_{th} hidden parameter. Theoretically this model can be an approximation of any nonlinear relationship. The size of the model does not grow exponentially with the number of inputs. Therefore the model can work in high dimension.

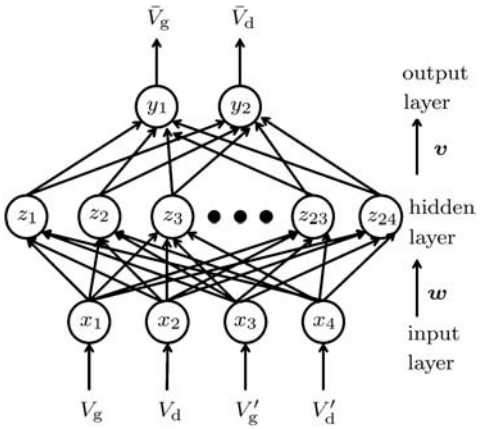


Fig. 3. A three-layer neural network.

The neural network learns the information from samples of input–output data, i.e. $\boldsymbol{v}_{\rm f}$ and $\boldsymbol{v}_{\rm c}$. During learning, the neural network automatically adjusts its weights and thresholds (i.e. w_{ih}, v_{hj} and θ_h) so that the error E between neural network predictions and sampled outputs

$$E = \frac{1}{2}\sum_{j=1}^{2}(V_{{\rm c}j} - y_j)^2 \quad (8)$$

is minimized. The adjustment equations are

$$w_{ih}^{\rm new} = w_{ih}^{\rm old} - \alpha\frac{\partial E}{\partial w_{ih}}, \quad (9)$$

$$v_{hj}^{\rm new} = v_{hj}^{\rm old} - \beta\frac{\partial E}{\partial v_{hj}}, \quad (10)$$

and

$$\theta_h^{\text{new}} = \theta_h^{\text{old}} - \gamma \frac{\partial E}{\partial \theta_h}, \tag{11}$$

where α, β and γ are positive constants that regulate the speed of learning. The learning algorithm we used is based on the multilayer error-correction learning.

5. Device modeling

We start with an EEHEMT model, which is developed with measured data and agilent IC-CAP software. And then an ANN model with neuro-SM is established based on the EEHEMT model. The neuro-SM maps the base voltage and the collector voltage onto the coarse model, and these mapped signals excite the coarse model, resulting in an improved value of the collector current. The neuro-SM technique is to use a novel formulation of space mapping to automatically modify the behaviour of existing device model so as to accurately match the behaviour of the new device. This is made possible by a neural network mapping, which modifies the voltage signal and current signal in the model as shown in Fig. 2. In this paper, the neuro-SM is used to model an AlGaN/GaN HEMT device with irregular nonlinear DC behaviour and S-parameters with multibiases.

Figure 4 shows the comparisons among the DC characteristics of measured data, calculated data from the EEHEMT model (without mapping) and those from the proposed ANN model (with mapping), with DC drain voltage ranging from 0 to 30 V and gate voltage from –7 to –2.5 V in steps of 0.45 V. From Fig. 4, it can be seen that the ANN model is more accurate than the EEHEMT model. This is because the neural network training can automatically adjust the mapping according to the needs of the specific coarse model. Figure 5 shows the forward transmission S_{21} from the measurements and the simulations from the EEHEMT model and the ANN model. Figure 5(a) shows the comparison between the simulated results from the EEHEMT model and the measured results. Figure 5(b) exhibits the comparison between the simulated results from the ANN model and the measured results.

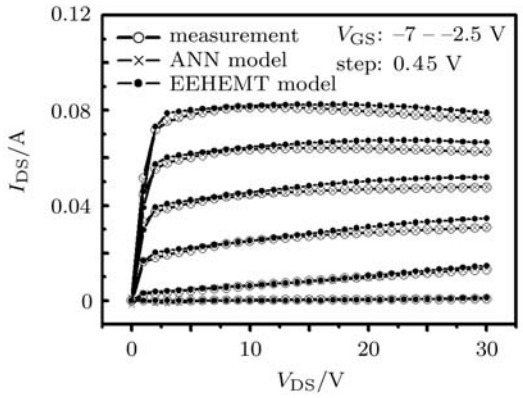


Fig. 4. Comparison of the device DC data: DC responses of the measurement data, the EEHEMT models (without mapping), and the Neuro-SM models (with mapping).

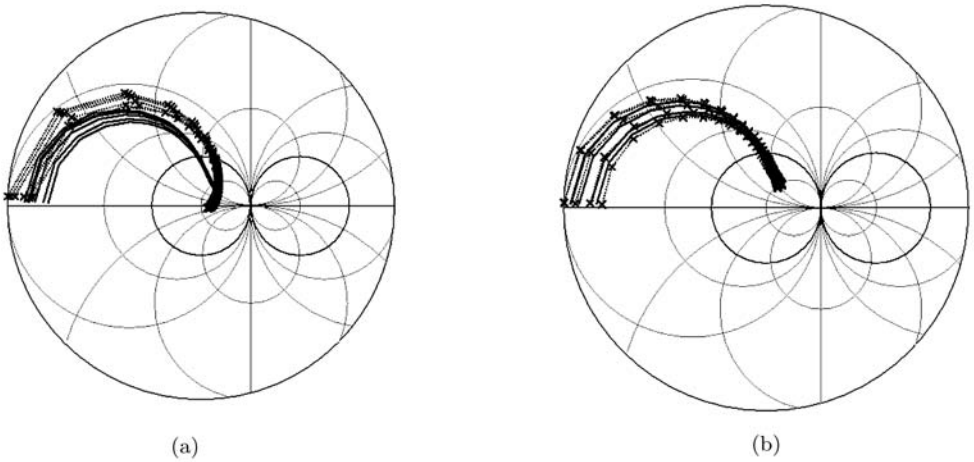


Fig. 5. Comparison of parameter S_{21} of the device (a) between simulated results from the EEHEMT model and measured data, and (b) between simulated results from the ANN model and measured data. Solid lines denote measured results and dot lines marked with symbol (×) denote simulated results.

Figure 6 shows the measured data and the simulated results of reverse transmission coefficient S_{12}, reflection coefficient of port 1 S_{11} and reflection coefficient of port 2 S_{22}. Figure 6(a) displays the comparison between the simulated results from the EEHEMT model and the measured results. Figure 6(b) gives the comparison between the simulated results from the ANN model with the measured results.

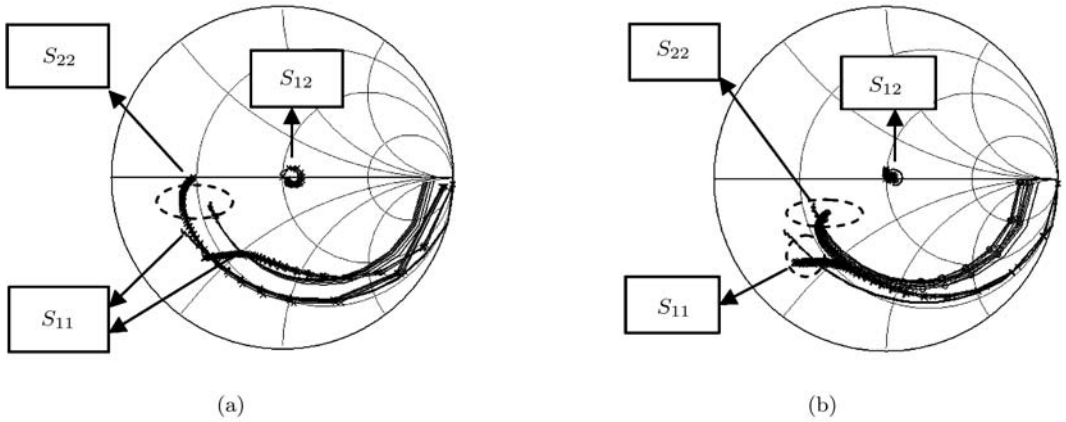


Fig. 6. Comparison among parameters S_{11}, S_{22} and S_{12} of device. (a) comparison between EEHEMT model simulated results and measured data, (b) comparison between ANN model simulated results and measured data. Solid lines denote measurement results and solid lines marked with symbol (×) denote simulated results.

The simulation conditions of two models are the same as the testing conditions in Figs. 5 and 6, i.e., frequency ranges from 50 MHz to 24.05 GHz in steps of 600 MHz, drain voltage is 6 V, and gate voltage ranges from –4.3 V to –2.5 V in steps of 0.45 V.

From Fig. 5, it is obvious that the matching between the simulated results from the ANN model and the measured data for S_{21} is much better than that between the simulated results from the EEHEMT model and the measured data for the whole frequency range. From Fig. 6, it can be seen that the matching between the simulated results from the ANN model and the measured data is better than that between the simulated results from the EEHEMT model and the measured data for S_{11}, S_{22}. The matching of S_{12} between the simulated results from the ANN model and the measured data is worse than that between the simulated results from the EEHEMT model and the measured data, but the difference is very small. In the neuro-SM, drain voltage, gate voltage and their first order derivative are used. Higher fitting accuracy may be achieved if the second order (or more) derivatives of drain voltage and gate voltage are included in the neuro-SM.

6. Conclusion

ANN modeling based on the EEHEMT model is applied to AlGaN/GaN HEMT for the first time. The accurate modeling based on the ANN model is achieved compared with the conventional EEHEMT modeling. It demonstrates that the ANN based modeling techniques can be applied to semiconductor device modeling and other complex situation modeling.

References

[1] Cheng Z Q, Liu J, Zhou Y G, Chen K J and Lau K M 2005 *IEEE Electron Device Letters* **26** 521
[2] Cheng Z Q, Cai Y, Liu J, Zhou G Y, Lau K M and Chen K J 2007 *Chin. Phys.* **16** 3494
[3] Cheng Z Q, Zhou X P, Hu S, Zhou W J and Zhang S 2010 *Acta Phys. Sin.* **59** 1252 (in Chinese)
[4] Wang T, Gao X D and Li W 2010 *Chin. Phys.* B **19** 070505
[5] Wang T, Wang A K, Yang Q W, Ding X T, Dong J Q, Sanuki H and Itoh K 2007 *Chin. Phys.* **16** 3738
[6] Zhang Q J, Gupta K C and Devabhaktuni V K 2003 *IEEE Trans. Microwave Theory Tech.* **51** 1339
[7] Bandler J W, Cheng Q S, Dakroury S, Mohamed A S, Bakr M H, Madsen K and Sondergaard J 2004 *IEEE Trans. Microwave Theory Tech.* **52** 337
[8] Steer M B, Bandler J W and Snowden C M 2002 *IEEE Trans. Microwave Theory Tech.* **50** 996
[9] Zhang L, Xu J J, Yanoub M C E, Ding R T and Zhang Q J 2005 *IEEE Trans. Microwave Theory Tech.* **53** 2752